Relativistic corrections of one-nucleon current in low-energy three-nucleon photonuclear reactions

A. Deltuva,[1] A. C. Fonseca,[1] and P. U. Sauer[2]

[1] *Centro de Física Nuclear da Universidade de Lisboa, P-1649-003 Lisboa, Portugal*
[2] *Institut für Theoretische Physik, Leibniz Universität Hannover, D-30167 Hannover, Germany*

(Received December 11, 2009)

Proton-deuteron radiative capture and two- and three-body photodisintegration of ^{3}He at low energy are described using realistic hadronic dynamics and including the Coulomb force. The sensitivity of the observables to the relativistic corrections of one-nucleon electromagnetic current operator is studied. Significant effects of the relativistic spin-orbit charge are found for the vector analyzing powers in the proton-deuteron radiative capture and for the beam-target parallel-antiparallel spin asymmetry in the three-body photodisintegration of ^{3}He.

PACS numbers: 25.20.-x, 21.45.-v, 24.70.+s, 25.40.Lw

I. INTRODUCTION

Electromagnetic (e.m.) reactions in the three-nucleon ($3N$) system have been extensively studied in the past aiming to test various models of the hadronic two-nucleon ($2N$) and $3N$ interaction and of the nuclear e.m. current [1–6]. In the nucleon-deuteron (Nd) radiative capture at higher energies [4] we observed quite a significant effect of the relativistic spin-orbit correction of the one-nucleon ($1N$) charge operator. This is consistent with the findings of Refs. [7–9] for the photodisintegration of the deuteron. However, quite surprisingly, we found sizable effect of the same relativistic spin-orbit correction also for the proton (p) and deuteron (d) vector analyzing powers in the low-energy pd radiative capture [10]. The aim of the present work is to calculate the observables of the low-energy $3N$ photonuclear reactions. For pd radiative capture we compare with existing data. For two- and three-body photodisintegration of ^{3}He we make predictions for experiments which are in the process of being performed at the HIGS facility [11]. We study the sensitivity of observables to relativistic corrections of the $1N$ charge and spatial current.

In Sec. II we describe the chosen model for the hadronic interaction and e.m. current. Selected results for the pd radiative capture and photodisintegration of ^{3}He are presented in Sec. III. We summarize in Sec. IV.

II. DYNAMICS

The hadronic dynamics is based on the realistic two-baryon coupled-channel potential CD Bonn + Δ [12] that allows for a virtual excitation of a nucleon to a Δ isobar and thereby yields effective many-nucleon forces [13]. The nonrelativistic part of the e.m. current is taken over from Ref. [4] and has one-baryon and two-baryon pieces. Beside the standard purely nucleonic part there are additional parts involving the Δ isobar which then make effective $2N$ and $3N$ contributions to the e.m. current that are consistent with the effective $2N$ and $3N$ forces. Since the underlying potential CD Bonn + Δ is based on the exchange of standard isovector mesons π and ρ and isoscalar mesons ω and σ, the same meson exchanges are contained in the effective nucleonic forces and currents. The initial and final $3N$ bound and scattering states are respectively described by the exact Faddeev and Alt, Grassberger, and Sandhas (AGS) three-particle equations [14] in the isospin formalism that are solved in momentum space using partial wave decomposition [15]. The Coulomb interaction between charged baryons is important in the considered low-energy reactions and is included using the method of screening and renormalization [16–18]. The current is expanded in electric and magnetic multipoles. The magnetic multipoles are calculated from the one- and two-baryon parts of the spatial current. The electric multipoles use the Siegert form of the current without the long-wavelength approximation; assuming current conservation, the dominant parts of the one-baryon convection current and of the diagonal π- and ρ-exchange current are taken into account implicitly in the Siegert part of the electric multipoles by the Coulomb multipoles of the charge density; the remaining non-Siegert part of the electric multipoles not accounted for by the charge density is calculated using explicit one- and two-baryon spatial currents. Although the continuity equation is not exactly fulfilled for the nonlocal potential CD Bonn + Δ or when the relativistic $1N$ current corrections are included, the employed calculational scheme, based on the Siegert form of the current, effectively corrects the current nonconservation as argued in Ref. [19] and is therefore reliable for the observables of low-energy photoreactions considered in this paper. We also note that the use of the nonrelativistic hadronic dynamics together with the relativistic current corrections is somehow inconsistent. However, in the low-energy reactions it is natural to expect the effect of the relativistic hadronic dynamics to be small; this expectation is consistent with the results of Ref. [20].

In order to isolate the effects of various relativistic current corrections we perform several calculations (all using CD Bonn + Δ as the hadronic potential and including

Coulomb) with a different choice of e.m. current:
(a) The nonrelativistic one- and two-baryon e.m. currents are used as in the standard calculations of Ref. [4], except for the parameters of the single nucleon-Δ transition current that are taken over from Ref. [21]. The corresponding results in the figures are given by the dashed-dotted curves.
(b) The relativistic spin-orbit correction to the $1N$ charge, as given by Eq. (A11a) of Ref. [4], is included in addition to (a); it contributes to the Siegert term. The corresponding results in the figures are given by the solid curves consistently with Ref. [10].
(c) With respect to the relativistic Darwin-Foldy correction to the $1N$ charge there is a controversy in the literature: according to Ref. [22] it vanishes identically for the reactions with real photons (γ) whereas it yields finite contribution according to Ref. [23]. We include the latter one in addition to (b), however, in all studied low-energy photoreactions its effect turns out to be entirely negligible and will therefore not be shown separately.
(d) In addition to (c) relativistic corrections to the $1N$ spatial current from Ref. [23] are included; they contribute to the magnetic multipoles and to the non-Siegert part of the electric multipoles. The corresponding results in the figures are given by the dotted curves.
(e) In addition to (d) the nucleon-Δ transition charge that is of the relativistic order as given by Eq. (A11b) of Ref. [4] is included. However, the corresponding results are not shown separately since the effect is entirely negligible.

The technical details of our calculations are explained in Refs. [4, 10, 24].

III. RESULTS

We start with the pd radiative capture where significant relativistic effects were predicted in Ref. [10]. In Fig. 1 we show the deuteron vector analyzing power $A_y(d)$ at deuteron lab energies $E_d = 10$, 17.5, and 29 MeV as a function of the center-of-mass (c.m.) $d-{}^3$He (or $p-\gamma$) scattering angle. The effect of the $1N$ spin-orbit charge is sizable and clearly improves the description of the experimental data whereas the relativistic corrections of the $1N$ spatial current contributing to the magnetic multipoles and to the non-Siegert part of the electric multipoles yield only minor changes. Furthermore, it is interesting to note that the spin-orbit charge effect increases with decreasing energy as the $A_y(d)$ itself does. A strong and beneficial effect is seen also in the proton analyzing power $A_y(p)$ at $E_p = 5$ MeV proton lab energy in Fig. 2. In contrast, the differential cross section and deuteron tensor analyzing powers at low energies remain almost unaffected by the spin-orbit charge as can be seen from our previous results [10] at $E_d = 6$ MeV; those results are not documented in this paper again. The spin-orbit charge effect shows up in the deuteron tensor analyzing powers as the energy increases, especially at forward and backward angles where the differential cross section is small. In Fig. 3 we show A_{yy} at $E_d = 45$ MeV; further examples can be found in Refs. [10, 27]. Finally we note that our nonrelativistic results, as documentad by the dashed-dotted curves, are consistent with the ones of Ref. [6] derived from the different hadronic interaction and e.m. current.

One may conjecture that large spin-orbit charge effect in low-energy $A_y(p)$ and $A_y(d)$ is due to the high momentum components present in the ^{3}He wave function. We therefore performed additional calculations with AV18 [28] and effective field theory N3LO [29] potentials that, although having quite comparable ^{3}He binding energies, 6.923 MeV and 7.128 MeV, respectively, differ significantly in the ^{3}He D-state probability, 8.47% and 6.32%, and in the expectation value for the ^{3}He internal kinetic energy, 45.68 MeV and 33.78 MeV. However, the spin-orbit charge effect turns out to be the same in both cases thereby ruling out the above conjecture. In fact, at low energy only the matrix elements $\langle {}^3\mathrm{He}|E1|pd({}^4P_J)\rangle$ with $J = \frac{1}{2}$ and $\frac{3}{2}$, i.e., the E1 transitions between the ${}^4P_J$ pd scattering states and the ^{3}He bound state, calculated using either the Siegert form (as in our standard procedure) or the explicit one- and two-baryon spatial currents, are significantly affected by the relativistic corrections. The nonrelativistic (spin-independent) charge contribution for these matrix elements is suppressed compared to the $\langle {}^3\mathrm{He}|E1|pd({}^2P_J)\rangle$ due to the total spin of the ^{3}He bound state being predominantly $\mathcal{S} = \frac{1}{2}$. As a consequence, the spin-orbit charge becomes important, especially for the $\langle {}^3\mathrm{He}|E1|pd({}^4P_{3/2})\rangle$ which is responsible for about 90% of the observed effect in the vector analyzing powers that are very sensitive to this particular matrix element.

For curiosity we show in Fig. 4 also the results at considerably higher energies, i.e., $E_p = 100$ MeV or $E_d = 200$ MeV, where not only the spin-orbit charge but also the relativistic corrections of the $1N$ spatial current yield visible effects for the differential cross section and spin observables. The description of the experimental data is quite satisfactory although in this energy regime one can expect further changes due to relativistic hadronic dynamics.

Next we consider the two-body photodisintegration of ^{3}He that is related to the pd radiative capture by time reversal. In Fig. 5 we present results for the linear photon asymmetry Σ, the target analyzing power $A_y({}^3\mathrm{He})$, and the beam-target parallel-antiparallel spin asymmetry A_{P-A}. The importance of the spin-orbit charge is different for these observables: Σ remains almost unaffected, $A_y({}^3\mathrm{He})$ shows moderate effect around the minimum whereas A_{P-A} is strongly affected but only at forward and backward angles where the differential cross section is small; the different effects are due to the different sensitivity of the observables to the crucial matrix elements $\langle {}^3\mathrm{He}|E1|pd({}^4P_J)\rangle$, as already encountered in the radiative capture. The effect of the relativistic corrections of the $1N$ spatial current is negligible for all con-

sidered ^{3}He photodisintegration observables and therefore will be not shown for the three-body breakup.

Finally in Figs. 6 and 7 we show our predictions for the semi-inclusive observables of the ^{3}He three-body photodisintegration. We note in passing that the inclusion of the Coulomb interaction for this reaction is — among all reactions considered in this paper — most important; that fact is also explicitly documented in Refs. [24, 32]. The inclusion of the spin-orbit charge yields no visible changes in the semi-inclusive differential cross section and in the spin observables Σ and $A_y(^3\mathrm{He})$ but leads to a significant effect for the asymmetry A_{P-A} that, in contrast to the two-body photodisintegration, is seen at *all* scattering angles of the detected proton or neutron. Note that the corresponding observable in the deuteron photodisintegration is affected by the relativistic $1N$ current corrections in a similar way [9].

IV. SUMMARY

We performed calculations of $3N$ photonuclear reactions at low energies and studied effects of various relativistic corrections to the $1N$ e.m. current operator. The spin-orbit charge is the only important correction when the Siegert form of the electric multipoles is used. The realistic coupled-channel potential CD Bonn + Δ with Coulomb and the corresponding e.m. current including relativistic $1N$ corrections are quite successful in accounting for the existing *pd* radiative capture data. Sizable and beneficial effects of the spin-orbit charge were found for proton and deuteron vector analyzing powers even at low energies where the corrections due to relativistic hadronic dynamics are expected to be small. With increasing energy the effect of the relativistic $1N$ current corrections becomes visible for other observables as well.

Among the observables of the two- and three-body photodisintegration of ^{3}He the beam-target parallel-antiparallel spin asymmetry A_{P-A} appears to be most sensitive to the relativistic $1N$ current corrections. Polarization data do not exist yet for these reactions but the corresponding experiments are under way at the HIGS facility. The upcoming data will provide crucial tests for the chosen hadronic and e.m. dynamics.

[1] J. Carlson and R. Schiavilla, Rev. Mod. Phys. **70**, 743 (1998).
[2] R. Skibiński, J. Golak, H. Kamada, H. Witała, W. Glöckle, and A. Nogga, Phys. Rev. C **67**, 054001 (2003).
[3] J. Golak, R. Skibiński, H. Witała, W. Glöckle, A. Nogga, and H. Kamada, Phys. Rep. **415**, 89 (2005).
[4] A. Deltuva, L. P. Yuan, J. Adam Jr., A. C. Fonseca, and P. U. Sauer, Phys. Rev. C **69**, 034004 (2004).
[5] V. D. Efros, W. Leidemann, G. Orlandini, and E. L. Tomusiak, Phys. Rev. C **69**, 044001 (2004).
[6] L. E. Marcucci, M. Viviani, R. Schiavilla, A. Kievsky, and S. Rosati, Phys. Rev. C **72**, 014001 (2005).
[7] A. Cambi, B. Mosconi, and P. Ricci, Phys. Rev. Lett. **48**, 462 (1982).
[8] F. Ritz, H. Arenhövel, and T. Wilbois, Few-Body Syst. **24**, 123 (1998).
[9] H. Arenhövel, Few-Body Syst. **26**, 43 (1999).
[10] A. Deltuva, A. C. Fonseca, and P. U. Sauer, Phys. Rev. C **71**, 054005 (2005).
[11] H. R. Weller, M. W. Ahmed, H. Gao, W. Tornow, Y. K. Wu, M. Gai, and R. Miskimen, Progr. Part. Nucl. Phys. **62**, 257 (2009).
[12] A. Deltuva, R. Machleidt, and P. U. Sauer, Phys. Rev. C **68**, 024005 (2003).
[13] A. Deltuva, A. C. Fonseca, and P. U. Sauer, Phys. Lett. B **660**, 471 (2008).
[14] E. O. Alt, P. Grassberger, and W. Sandhas, Nucl. Phys. **B2**, 167 (1967).
[15] A. Deltuva, K. Chmielewski, and P. U. Sauer, Phys. Rev. C **67**, 034001 (2003).
[16] J. R. Taylor, Nuovo Cimento B **23**, 313 (1974); M. D. Semon and J. R. Taylor, Nuovo Cimento A **26**, 48 (1975).
[17] E. O. Alt and W. Sandhas, Phys. Rev. C **21**, 1733 (1980).
[18] A. Deltuva, A. C. Fonseca, and P. U. Sauer, Annu. Rev. Nucl. Part. Sci. **58**, 27 (2008).
[19] A. Deltuva, Ph.D. thesis, University of Hannover, 2003, http://edok01.tib.uni-hannover.de/edoks/e01dh03/374454701.pdf.
[20] H. Witała, J. Golak, R. Skibiński, W. Glöckle, W. N. Polyzou, and H. Kamada, Phys. Rev. C **77**, 034004 (2008).
[21] A. Deltuva, L. P. Yuan, J. Adam Jr., and P. U. Sauer, Phys. Rev. C **70**, 034004 (2004).
[22] J. L. Friar, B. F. Gibson, and G. L. Payne, Phys. Rev. C **30**, 441 (1984).
[23] F. Ritz, H. Göller, T. Wilbois, and H. Arenhövel, Phys. Rev. C **55**, 2214 (1997).
[24] A. Deltuva, A. C. Fonseca, and P. U. Sauer, Phys. Rev. C **72**, 054004 (2005).
[25] H. Akiyoshi, K. Sagara, S. Ueno, N. Nishimori, T. Fujita, K. Maeda, H. Nakamura, and T. Nakashima, Phys. Rev. C. **64**, 034001 (2001).
[26] F. Goeckner, W. K. Pitts, and L. D. Knutson, Phys. Rev. C **45**, R2536 (1992).
[27] T. Klechneva *et al.*, Phys. Rev. C **73**, 034005 (2006).
[28] R. B. Wiringa, V. G. J. Stoks, and R. Schiavilla, Phys. Rev. C **51**, 38 (1995).
[29] D. R. Entem and R. Machleidt, Phys. Rev. C **68**, 041001(R) (2003).
[30] M. A. Pickar, H. J. Karwowski, J. D. Brown, J. R. Hall, M. Hugi, R. E. Pollock, V. R. Cupps, M. Fatyga, and A. D. Bacher, Phys. Rev. C **35**, 37 (1987).
[31] T. Yagita *et al.*, Mod. Phys. Lett. **A18**, 322 (2003).
[32] A. Deltuva, A. C. Fonseca, and P. U. Sauer, Nucl. Phys. **A790**, 344c (2007).

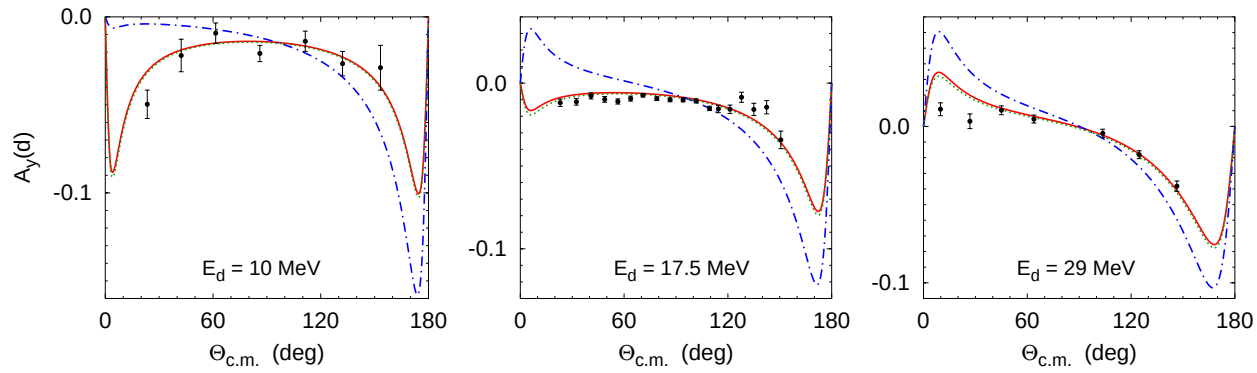

FIG. 1. (Color online) Deuteron vector analyzing power $A_y(d)$ for pd radiative capture at $E_d = 10$, 17.5, and 29 MeV as function of the c.m. $d - {}^3$He scattering angle. Results obtained with nonrelativistic e.m. current (dashed-dotted curves), including relativistic spin-orbit charge (solid curves), and including in addition relativistic corrections to the spatial current (dotted) curves are compared with the experimental data from Refs. [25–27].

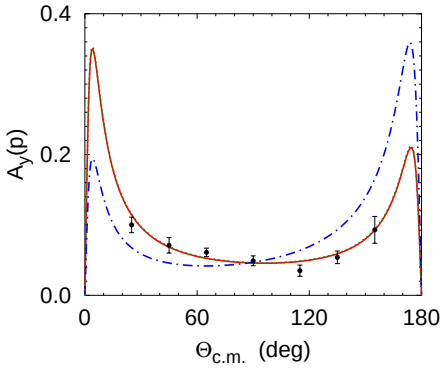

FIG. 2. (Color online) Proton vector analyzing power $A_y(p)$ for pd radiative capture at $E_p = 5$ MeV as function of the c.m. $p - \gamma$ scattering angle. Curves as in Fig. 1 and the experimental data are from Ref. [26].

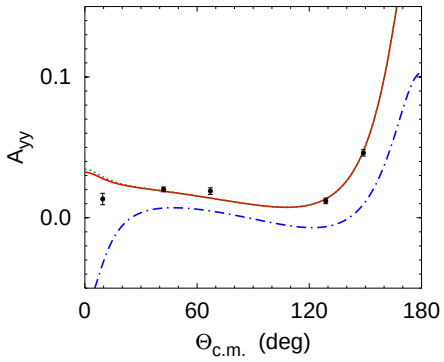

FIG. 3. (Color online) Deuteron tensor analyzing power A_{yy} for pd radiative capture at $E_d = 45$ MeV as function of the c.m. $d - {}^3$He scattering angle. Curves as in Fig. 1 and the experimental data are from Ref. [27].

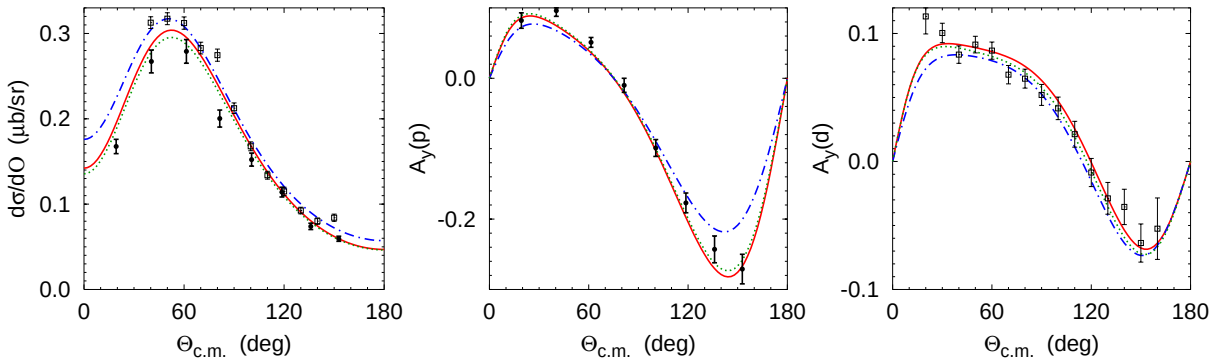

FIG. 4. (Color online) Observables of pd radiative capture at $E_p = 100$ MeV as functions of the c.m. $p-\gamma$ scattering angle. Curves as in Fig. 1 and the experimental data are from Refs. [30] (full circles) and [31] (open squares).

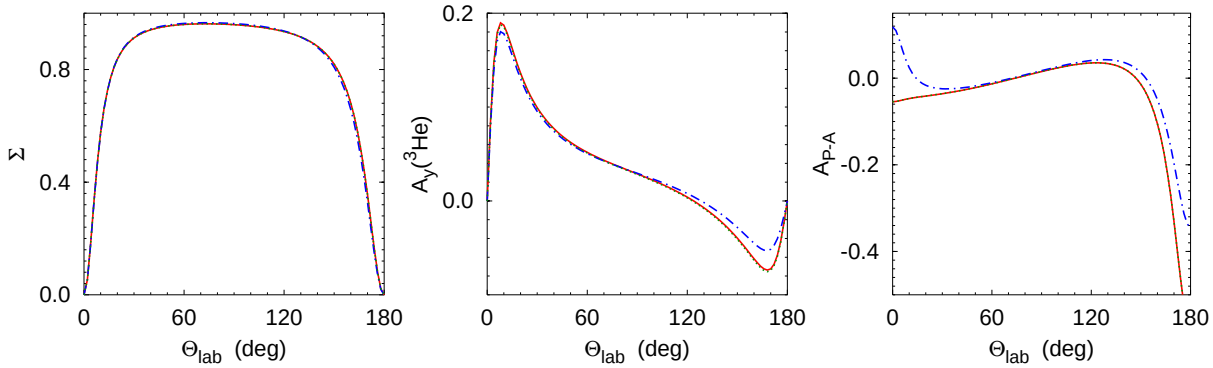

FIG. 5. (Color online) Observables of ^{3}He two-body photodisintegration at $E_\gamma = 15.2$ MeV as functions of the lab $\gamma - p$ scattering angle. Curves as in Fig. 1.

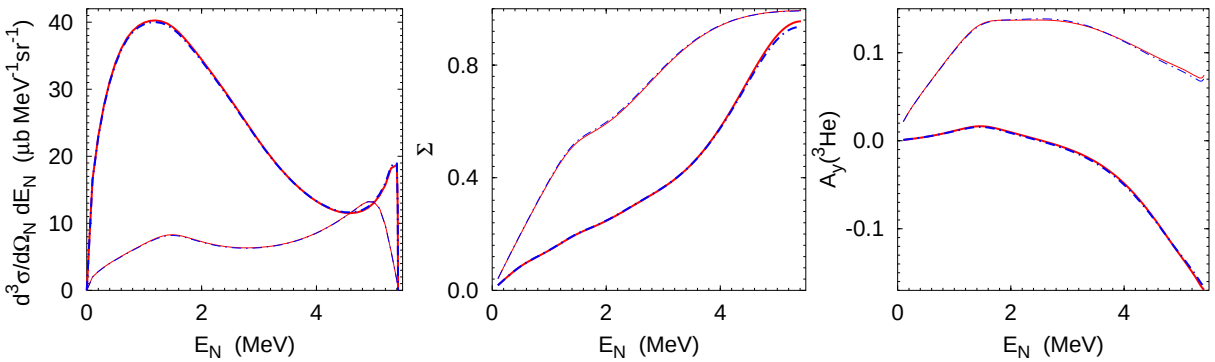

FIG. 6. (Color online) Observables of ^{3}He three-body photodisintegration at $E_\gamma = 15.2$ MeV as functions of the detected nucleon lab energy for the nucleon lab scattering angle $\Theta_N = 30°$. Results obtained with nonrelativistic e.m. current are given by thick (thin) dashed-dotted curves for the detected proton (neutron) whereas the results including relativistic spin-orbit charge are given by thick (thin) solid curves for the detected proton (neutron). Solid and dashed-dotted curves lie almost on top of each other.

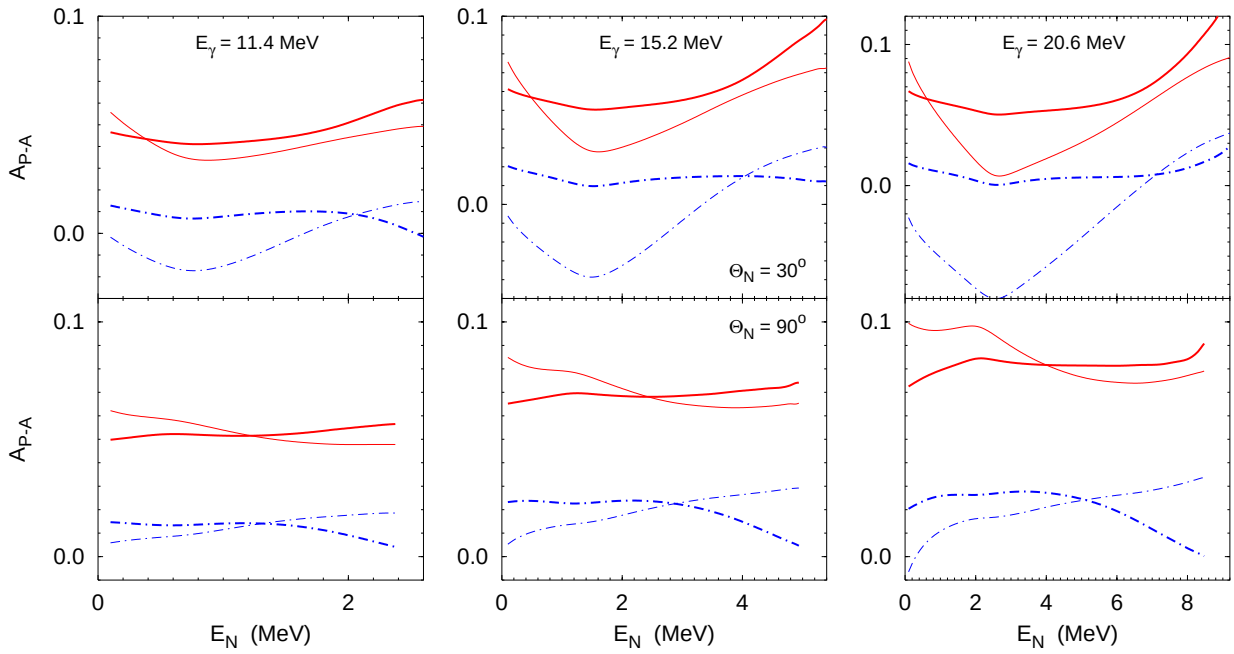

FIG. 7. (Color online) Parallel-antiparallel asymmetry of ^{3}He three-body photodisintegration at $E_\gamma = 11.4$, 15.2, and 20.6 MeV as function of the detected nucleon lab energy for $\Theta_N = 30^\circ$ (top) and 90° (bottom). Curves as in Fig. 6.